

Reconstruction of the heat transfer coefficient in the problem of binary alloy solidification with application of the broken line model

D. Słota*, E. Hetmaniok, R. Witula

Institute of Mathematics, Silesian University of Technology, Kaszubska 23, 44-100 Gliwice, Poland

*Corresponding author. E-mail address: damian.slota@polsl.pl

Received 13.06.2011; accepted in revised form 27.07.2011

Abstract

In the paper, solution of the inverse problem is presented, which consists in determination of the heat transfer coefficient during the process of binary alloy solidification for the known temperature measurements in the selected points of the cast. In the considered model distribution of temperature is described with the aid of Stefan problem with the varying liquidus temperature depending on the concentration of alloy component. Whereas, for description of the concentration the broken line model is used.

Keywords: Application of information technology to the foundry industry, Solidification, Heat transfer, Macroseggregation

1. Formulation of the problem

In the considered model distribution of temperature is described by using the Stefan problem [4] with the varying temperature at the beginning of solidification process, depending on the concentration of alloy component. Whereas, for describing the concentration will we apply the broken line model [3,7,9,10]. Problem under consideration consists in determining the value of heat transfer coefficient for the known measurements of temperature in the selected points of the cast.

In the region Ω , taken by the solidifying material, two varying in time subregions are considered: region Ω_1 , taken by the liquid phase, and region Ω_2 , taken by the solid phase (Fig. 1). Those two subregions are divided by the freezing front Γ_g , defined by the liquidus temperature varying in time (or by the, so called, substitute

solidification temperature [3,4]). Distribution of temperature in each phase is defined by means of the heat conduction equation ($i = 1, 2$):

$$c_i \rho_i \frac{\partial T_i}{\partial t}(x, t) = \lambda_i \frac{\partial^2 T_i}{\partial x^2}(x, t), \quad (1)$$

for $x \in \Omega_i$, $t \in (0, t^*)$, where c_i , ρ_i and λ_i denote, respectively, the specific heat, mass density and thermal conductivity in liquid phase ($i = 1$) and solid phase ($i = 2$), while t and x refer to the time and spatial location. On the boundary Γ_0 the initial condition is given ($T_0 > T^*(Z_0)$):

$$T_i(x, 0) = T_0, \quad (2)$$

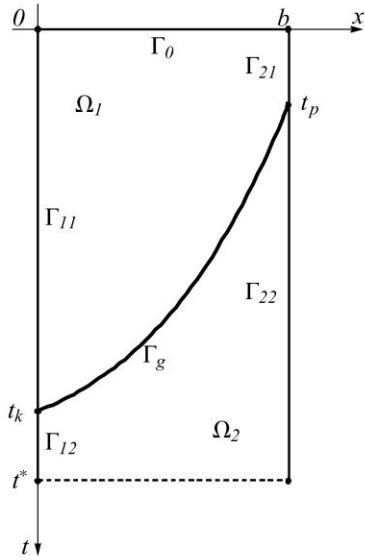


Fig. 1. Domain of the problem

where T_0 is the initial temperature, T^* is the temperature of beginning of the solidification process, Z_0 is the initial concentration of the alloy component. On boundaries Γ_{1i} ($i=1,2$) the homogeneous boundary conditions of the second kind are defined:

$$\frac{\partial T_i}{\partial x}(x,t) = 0, \quad (3)$$

whereas on boundaries Γ_{2i} ($i=1,2$) the boundary conditions of the third kind are determined:

$$-\lambda_i \frac{\partial T_i}{\partial x}(x,t) = \alpha(t)(T_i(x,t) - T_\infty), \quad (4)$$

where α is the heat transfer coefficient, T_∞ is the ambient temperature. On the freezing front Γ_g the condition of temperature continuity and the Stefan condition are given:

$$T_1(\xi(t), t) = T_2(\xi(t), t) = T^*(Z_L(t)), \quad (5)$$

$$L \rho_2 \frac{d\xi(t)}{dt} = -\lambda_1 \left. \frac{\partial T_1(x,t)}{\partial x} \right|_{x=\xi(t)} + \lambda_2 \left. \frac{\partial T_2(x,t)}{\partial x} \right|_{x=\xi(t)}, \quad (6)$$

where T^* is the temperature of beginning of the solidification process, $Z_L(t)$ denotes the concentration of the alloy component on the freezing front in the liquid phase side, L is the latent heat of fusion and $\xi(t)$ describes the location of freezing front.

In the broken line model [3,9,10] (which can be considered as the special case of the Burton, Prim and Slichter model [1]) it is assumed that the concentration of alloy component in the liquid phase can be

approximated by the broken line, in such a way that in the layer (of the width equal to δ) located close to the freezing front the distribution of concentration of the alloy component is described by the increasing (or decreasing) linear function. Whereas, in remaining part of the liquid phase the distribution of concentration of the alloy component is constant. In the solid phase it is assumed that $D_2 = 0$ (thus, diffusion in solid phase is ignored), which means that the concentration of alloy component in this phase is a consequence of the partition coefficient. By introducing the discretization of the interval $[0, t^*]$ with the nodes t_i , $i = 0, 1, \dots, n$, we can determine the relation defining the approximate value of concentration of alloy component on the freezing front in the liquid phase side (see [7]):

$$Z_L(t_{p+1}) = \frac{1}{\xi_{p+1} + \frac{1}{2} h_p k} \left(Z_0 b + \delta m_{p+1} \xi_{p+1} - \frac{1}{2} \delta^2 m_{p+1} - \sum_{i=1}^{p-1} \left(\frac{Z_S(t_i) - Z_S(t_{i+1})}{2} h_i \right) - \frac{Z_S(t_p)}{2} h_p \right), \quad (7)$$

where $m_i = m(t_i)$, $\xi_i = \xi(t_i)$, $h_i = \xi(t_{i+1}) - \xi(t_i)$.

In the considered inverse problem for the given values of temperature:

$$T(x_i, t_j) = U_{ij}, \quad (8)$$

for $i=1, 2, \dots, N_1$, $j=1, 2, \dots, N_2$, where N_1 denotes the number of sensors and N_2 describes the number of measurements from each sensor, determination of the value of heat transfer coefficient α is desired. For the given value of heat transfer coefficient the above problem turns into the direct problem, solving of which enables to find the courses of temperature $T_{ij} = T(x_i, t_j)$. By using the calculated values of temperature T_{ij} and the known values of temperature U_{ij} we can formulate the functional determining the error of approximate solution:

$$J(\alpha) = \sum_{i=1}^{N_1} \sum_{j=1}^{N_2} (T_{ij} - U_{ij})^2. \quad (9)$$

2. Method of solution

Direct Stefan problem (equations (1)-(6) for the known value of heat transfer coefficient) is solved by using the finite element method with the aid of alternating phase truncation method [2,5,8]. Approximate position of the freezing front in moment t_{p+1} is determined in such a way that there are calculated two points: the last point of the liquid phase, that is the point x_i in which $T(x_i, t_{p+1}) \geq T^*(Z_L(t_p))$, and the first point of the solid phase, that is the point x_j in which $T(x_j, t_{p+1}) < T^*(Z_L(t_p))$. Next, the position of freezing front ξ_{p+1} is determined by interpolating

linearly the points $(x_i, T(x_i, t_{p+1}))$ and $(x_j, T(x_j, t_{p+1}))$, and by evaluating value of the argument in which the interpolating function takes the value $T^*(Z_L(t_p))$. Velocity of the freezing front is determined by using the Stefan condition (6). Afterwards, basing on the formula (7), value $Z_L(t_{p+1})$ of the concentration of alloy component at moment t_{p+1} is calculated which determines the new value of solidification temperature $T^*(Z_L(t_{p+1}))$.

For finding minimum of the functional (9) the genetic algorithm is applied. In calculations, the floating-point (real) coding and the tournament selection is used. Moreover, the elitist model is applied in which the best individual of previous generation is remembered and, if all individuals in the current generation are worse, then the worst of them is replaced by the remembered best individual from the previous generation. The arithmetical crossover and the nonuniform mutation [5,6,8] are also used in the work. Finally, the calculations are made for the following values of parameters of the genetic algorithm: size of population $n_{pop} = 100$, number of generations $N = 100$, crossover probability $p_c = 0.7$ and mutation probability $p_m = 0.1$.

3. Numerical example

In the example the alloy Cu-Zn (10% Zn) [3,7] is considered. We assume that in the considered region three thermocouples are placed ($N_1 = 3$) in the distance of 8, 16 and 24 mm away from the external border of region. Readings of temperature are taken at every 0.1, 0.5 and 1 s. In calculations we use the exact values of temperature and the values burdened with the random error of magnitude 1, 2 and 5%.

In Table 1 the results of reconstruction of the sought parameters are compiled. Presented results are received for the exact input data and for various numbers of measurement points. Table 1 shows the mean values of reconstructed parameters α_i (calculated for 15 runs of the algorithm for different settings of the pseudo-random number generator), the relative percentage errors and standard deviation of this of reconstruction. It can be seen that in each case the boundary conditions are very well reconstructed. In case of the exact input data the maximal error of the sought parameters reconstruction does not exceed the value of 0.009%. Successive runs of the algorithm gave similar results which are confirmed by the small value of standard deviation.

In Figures 2 and 3 the errors of the sought parameters reconstruction, in case of the perturbed input data, are compiled. Figure 2 present the results obtained for temperature measurements taken at every 1 s and for various values of input data perturbation. Whereas, Figure 3 display the results received for the input data perturbation of the values 5% and for the various numbers of control points (measurements of temperature taken at every 0.1, 0.5 and 1 s). It can be noticed that in each case the errors of boundary condition reconstruction (calculated for the burdened input data) are smaller than the errors of input data. In case of the smallest number of measurement points and the perturbation value of 1% the errors do not exceed 0.11%, for the perturbation value of 2% the errors do not exceed 0.84%, while

for the perturbation value of 5% the errors do not exceed 0.52%. In case of the temperature measurements at every 0.5 s the errors are not greater than the values of 0.31, 0.32 and 0.56%, respectively. Finally, for the biggest number of measurement points the errors do not exceed the values 0.07, 0.19 and 0.62%, respectively.

Table 1.

Results of the sought parameters reconstruction for the exact input data and for the various number of measurement points (σ - standard deviation)

α_i	Error [%]	σ
0.1 s		
1199.98	0.0014	0.0971
800.03	0.0039	0.1330
249.99	0.0049	0.0320
0.5 s		
1199.97	0.0027	0.2108
800.01	0.0018	0.0950
250.00	0.0000	0.0179
1.0 s		
1199.93	0.0059	0.2076
800.07	0.0085	0.1630
249.99	0.0049	0.0322

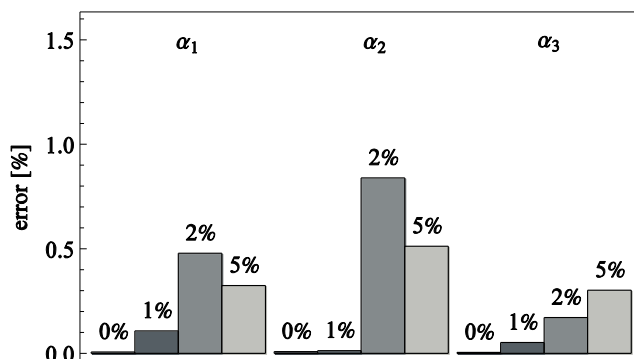


Fig. 2. Relative errors of the reconstructed heat transfer coefficient calculated for the various values of input data disturbances and temperature measurements taken at every 1 s

Standard deviation of received results is small in general, but the biggest value is taken for the biggest perturbation of input data (5%). In case of the 5% perturbation and measurements of temperature taken at every 0.1 s the standard deviation of reconstructed values of parameters α_i , $i = 1, 2, 3$ is equal to 0.6431, 0.4047 and 0.0409, respectively. For temperature measurements read at every 0.5 s the standard deviation is at the level of 9.3825, 4.3958 and 0.2144, respectively. And finally for readings of temperature made at every 1 s the standard deviation is equal to 3.9638, 1.7035 and 0.1142, respectively. In the rest of cases the values of standard deviation are smaller.

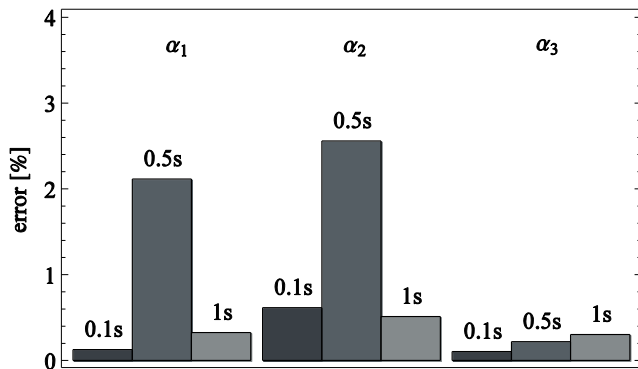


Fig. 3. Relative errors of the reconstructed heat transfer coefficient obtained for the various number of temperature measurements (calculations are made for the input data burdened by the 5% error)

Table 2.

Errors of reconstruction of temperature in the control points (Δ_{mean} - mean value of the absolute error, Δ_{max} - maximal value of the absolute error, δ_{mean} - mean value of the relative error, δ_{max} - maximal value of the relative error)

Perturbation	0%	1%	2%	5%
0.1 s				
Δ_{mean} [K]	0.0027	0.0272	0.1127	0.1252
Δ_{max} [K]	0.0135	1.2192	1.4168	2.9192
δ_{mean} [%]	0.0002	0.0022	0.0093	0.0102
δ_{max} [%]	0.0010	0.0936	0.1091	0.2243
0.5 s				
Δ_{mean} [K]	0.0007	0.0621	0.1428	0.3591
Δ_{max} [K]	0.0287	0.4484	5.0798	8.1755
δ_{mean} [%]	0.0001	0.0051	0.0116	0.0293
δ_{max} [%]	0.0022	0.0368	0.3902	0.6252
1.0 s				
Δ_{mean} [K]	0.0032	0.0287	0.1434	0.1973
Δ_{max} [K]	0.0652	1.3116	5.0808	5.0798
δ_{mean} [%]	0.0003	0.0023	0.0118	0.0162
δ_{max} [%]	0.0050	0.1010	0.3903	0.3903

In Table 2 the errors of temperature reconstruction in the control points are compiled. It can be seen that the distribution of temperature is reconstructed very well in each case. For the exact input data the maximal absolute error of the temperature reconstruction does not exceed 0.07 K, whereas the mean absolute

error is not greater than 0.0032 K (the relative errors are equal to: 0.005% - the maximal and 0.0003% - the mean one). The biggest errors of temperature reconstruction are noticed for temperature measurements taken at every 0.5 s and input data perturbed by the error of 5%. In this case the maximal absolute error does not exceed 8.18 K and the mean absolute error is not bigger than 0.36 K, whereas the relative errors are at the level of: 0.6252% - the maximal and 0.0293% - the mean one.

4. Conclusions

Presented algorithm enables to determine the missing boundary condition in the problem of binary alloy solidification. Executed calculations show that the unknown heat transfer coefficient is very well reconstructed. Algorithm is stable with regard to the errors of input data. Moreover, received results indicate that increase of the number of control points or decrease of the value of input data errors cause more precise reconstruction of the sought parameters and, in this way, better reconstruction of the exact temperature distribution.

References

- [1] J.A. Burton, R.C. Prim, W.P. Slichter, The distribution of solute in crystal grown from the melt. Part I theoretical, Journal of Chemical Physics, vol. 21 (1953), 1987-1991.
- [2] E. Majchrzak, B. Mochnacki, Application of the BEM in the thermal theory of foundry, Engineering Analysis with Boundary Elements, vol. 16 (1995), 99-121.
- [3] B. Mochnacki, E. Majchrzak, R. Szopa, Simulation of heat and mass transfer in domain of casting made from binary alloy, Archives of Foundry Engineering, vol. 8 (4) (2008), 121-126.
- [4] B. Mochnacki, J.S. Suchy, Numerical Methods in Computations of Foundry Processes, PFTA, Cracow 1995.
- [5] D. Słota, Solving the inverse Stefan design problem using genetic algorithms, Inverse Problems in Science and Engineering, vol. 16 (2008), 829-846.
- [6] D. Słota, Identification of the cooling condition in 2-D and 3-D continuous casting processes, Numerical Heat Transfer Part B, vol. 55 (2009), 155-176.
- [7] D. Słota, Estimation of the thickness of boundary layer in a broken line model of binary alloy solidification, Archives of Foundry Engineering, vol. 10, sp. is. 4 (2010), 79-82.
- [8] D. Słota, Restoring boundary conditions in the solidification of pure metals, Computers & Structures, vol. 89 (2011), 48-54.
- [9] J.S. Suchy, B. Mochnacki, Analysis of segregation process using the broken line model. Theoretical base, Archives of Foundry, vol. 3, no. 10 (2003), 229-234.
- [10] J.S. Suchy, B. Mochnacki, M. Prazmowski, Analysis of segregation process using the broken line model. Numerical realization, Archives of Foundry, vol. 3, no. 10 (2003), 235-240.